Scenario simulation of water retention services under land use/cover and climate changes: a case study of the Loess Plateau, China

SUN Dingzhao[1,2,3], LIANG Youjia[2*], PENG Shouzhang[1]

[1] State Key Laboratory of Soil Erosion and Dryland Farming on the Loess Plateau, Institute of Water and Soil Conservation, Chinese Academy of Sciences and Ministry of Water Resources, Yangling 712100, China;
[2] School of Resources and Environmental Engineering, Wuhan University of Technology, Wuhan 430070, China;
[3] Institute of Surveying and Mapping, Guizhou Geology and Mineral Exploration Bureau, Guiyang 550018, China

Abstract: Comprehensive assessments of ecosystem services in environments under the influences of human activities and climate change are critical for sustainable regional ecosystem management. Therefore, integrated interdisciplinary modelling has become a major focus of ecosystem service assessment. In this study, we established a model that integrates land use/cover change (LUCC), climate change, and water retention services to evaluate the spatial and temporal variations of water retention services in the Loess Plateau of China in the historical period (2000–2015) and in the future (2020–2050). An improved Markov-Cellular Automata (Markov-CA) model was used to simulate land use/land cover patterns, and ArcGIS 10.2 software was used to simulate and assess water retention services from 2000 to 2050 under six combined scenarios, including three land use/land cover scenarios (historical scenario (HS), ecological protection scenario (EPS), and urban expansion scenario (UES)) and two climate change scenarios (RCP4.5 and RCP8.5, where RCP is the representative concentration pathway). LUCCs in the historical period (2000–2015) and in the future (2020–2050) are dominated by transformations among agricultural land, urban land and grassland. Urban land under UES increased significantly by 0.63×10^3 km²/a, which was higher than the increase of urban land under HS and EPS. In the Loess Plateau, water yield decreased by 17.20×10^6 mm and water retention increased by 0.09×10^6 mm in the historical period (2000–2015), especially in the Interior drainage zone and its surrounding areas. In the future (2020–2050), the pixel means of water yield is higher under RCP4.5 scenario (96.63 mm) than under RCP8.5 scenario (95.46 mm), and the pixel means of water retention is higher under RCP4.5 scenario (1.95 mm) than under RCP8.5 scenario (1.38 mm). RCP4.5-EPS shows the highest total water retention capacity on the plateau scale among the six combined scenarios, with the value of 1.27×10^6 mm. Ecological restoration projects in the Loess Plateau have enhanced soil and water retention. However, more attention needs to be paid not only to the simultaneous increase in water retention services and evapotranspiration but also to the type and layout of restored vegetation. Furthermore, urbanization needs to be controlled to prevent uncontrollable LUCCs and climate change. Our findings provide reference data for the regional water and land resources management and the sustainable development of socio-ecological systems in the Loess Plateau under LUCC and climate change scenarios.

Keywords: water retention; water yield; land use/cover change; climate change; representative concentration pathway; Markov-Cellular Automata model; Loess Plateau

1 Introduction

Ecosystem services refer to the benefits that humans derive directly or indirectly from ecosystems (Costanza et al., 1997). Ecosystem services assessment frameworks such as Millennium Ecosystem Assessment and Economics of Ecosystems and Biodiversity (TEEB) Programs emphasizing the close relationship between ecosystems and human well-being, have greatly advanced ecosystem services research (Perrings et al., 2011). With the application of ecosystem services research on a global scale, numerous countries and government organizations have utilized it in the formulation of development policies and the rational allocation methods of natural resources, which are projected to be the long-term trends in ecosystem services research pertaining to the global sustainable development (Bai et al., 2019).

Water retention services are defined as the capacity of an ecosystem to intercept and store precipitation, which reflects the sustainability of regional water resources to a certain extent (Bai et al., 2011; Quintas-Soriano et al., 2014). Water retention services are key factors determining the continuous supply of regional water resources and regional development (Feng et al., 2016a; Hackbart et al., 2017). On a large spatial-temporal scale, land use and climate change are the major factors inducing the changes in water retention services (Su and Fu, 2013; van Vliet, 2019), however, the processes and methods of these influences are complex, especially in the future, with uncertainties. A large number of studies have attempted to investigate the mechanisms underlying these relationships and quantify the influencing processes, in order to support regional ecological construction and sustainable development (He et al., 2019; Wen and Théau, 2020; Hu et al., 2021; Wang et al., 2021).

Since the 20th century, large-scale urban expansion and vegetation restoration have been the main land use/cover changes (LUCCs) in China. Over the past 30 a, the Loess Plateau in China underwent vigorous urbanization, with an urbanization rate of approximately 30% in the whole Loess Plateau, while the urbanization rate of cities is about 80% such as Xi'an (Wu et al., 2019). Studies have shown that rapid urbanization, a global phenomenon, has significantly changed the relationship among atmosphere, hydrosphere, and biosphere, leading to a decrease in regional water storage and the expansion of rural settlements (Li et al., 2016). Furthermore, the expansion of construction land that performs at the expense of ecological lands, such as cultivated land, forest land, and grassland (Peng et al., 2016), is the direct cause of the decline in ecosystem services such as water yield. However, population accumulation and economic development are the indirect causes of the decline in ecosystem services (Peng et al., 2017). Meanwhile, a series of vegetation restoration and protection measures have been taken for promoting soil-water retention services in the Loess Plateau, such as the Grain for Green Project (GGP), the Natural Forest Protection Project (NFPP), and the Three-North Shelter Forest Program (TNSFP), which have markedly increased the vegetation cover in the region (Chen et al., 2015). Su and Fu (2013) pointed out that during 1975–2008 in the Loess Plateau, the areas of woodland and grassland increased by 0.47×10^4 and 1.90×10^4 km^2, respectively, while the area of farmland decreased by 2.5×10^4 km^2. Especially after the implementation of the GGP (2000–2008), a large area of steep slope farmland was converted into grassland and woodland. On the other hand, vegetation restoration exerts negative effects on water retention as well. For instance, LUCC caused by the GGP has decreased water yield by 38% in the Loess Plateau (Feng et al., 2012). Furthermore, 0.09×10^6 km^2 land that changed following the implementation of the GGP during 2000–2015, has resulted in a decrease of runoff by 1.5×10^9 m^3 in the Loess Plateau (Deng et al., 2019). Therefore, vegetation restoration requires appropriate trade-offs and optimized management in the Loess Plateau.

Water retention services are directly affected by precipitation in the Loess Plateau and tend to be more sensitive to climate change than those in other global regions (Jiang et al., 2018).

Numerous studies have attempted to reveal the significant changes of water retention services in the Loess Plateau, a region that has been under a warming and drying climate trend over the past 30 a (e.g., Zhou et al., 2005; Su and Fu, 2013; Fu et al., 2017). Feng et al. (2016b) pointed out that the average runoff decreased gradually from 1961 to 2009 at a rate of 0.9 mm/a in the Loess Plateau; they attributed this phenomenon to a decrease of precipitation. Fu et al. (2017) reported that the decrease of precipitation is the key factor influencing the decrease of the Yellow River runoff in the Loess Plateau. The Loess Plateau occupies a vast area, so its key elements such as land use and climate are heterogeneous in geographic space. Clarifying the spatial characteristics and trends of land use and climate change and quantifying their impacts on water retention services are indispensable for reviewing and summarizing the suitability of existing development models and exploring future sustainable development paths in the Loess Plateau.

Spatially explicit modelling under scenarios is a useful method for quantifying the impacts of land use and climate change on ecosystem services (Martnez-Harms and Balvanera, 2012; Kim et al., 2013; Hu et al., 2020). Among modelling tools of ecosystem services, the integrated valuation of ecosystem services and tradeoffs (InVEST) model is the most commonly used approach for reflecting the impacts of land use and climate change on hydrological processes at multi-scales. However, the model is used as a "black box" due to non-spatial input parameters, which simplify the evaluation process to a certain extent, yet bringing difficulty to parameter verification (Ochoa and Urbina-Cardona, 2017; Chen et al., 2018; Kim and Jung, 2020). Spatial input parameters could provide better feedback than non-spatial input parameters, considering the spatial variability of climatic and geographic attributes at large scales in the Loess Plateau. Spatially explicit modelling using Markov-Cellular Automata (Markov-CA) model is increasingly being applied for multi-scenario spatial-temporal simulations of future land use at regional scales (Du et al., 2020). In this study, the future land use demand was calculated using Markov model, which is based on the initial state probability matrix formed by land use in two periods (Muller and Middleton, 1994; Guan et al., 2011). Future land use simulation (FLUS) model, a typical CA model, was used for reflecting land supply and differences in actual land use changes. FLUS model integrates artificial neural network (ANN) algorithm and roulette wheel selection (RWS) mechanism (Liu et al., 2017) and is extensively used in multi-scenario land use simulations with high accuracy (Liang et al., 2018; Lin et al., 2020).

In this study, we aimed to comprehensively understand the nexus relationship between land use and water retention services in the Loess Plateau using integrated modelling methods. Markov model was first modified to simulate multi-scenario land use demands and then integrated with ANN-based suitability probability estimation (ANN-SPE) and self-adaptive inertia and competition mechanism (SAICM) modules of FLUS model to calculate the probabilities of occurrence for different land use types and their pattern variations. Subsequently, a spatially explicit water retention services model was developed using ArcGIS 10.2 (ESRI, Redlands, California, USA).

More specifically, the main objectives of this study are to: (1) develop an integrated modelling framework, including modified Markov-FLUS, water retention assessment model, and multi-source datasets via various mapping techniques; (2) simulate the spatial-temporal variations in land use types and water retention services in the Loess Plateau in the historical period (2000–2015); (3) define land use scenarios of historical scenario (HS), ecological protection scenario (EPS), and urban expansion scenario (UES), and obtain climate products under RCP4.5 and RCP8.5 (RCP, representative concentration pathway)scenarios (IPCC, 2017) in the simulation period (2020–2050); (4) determine the spatial-temporal variations in water retention services based on different combinations of aforementioned land use and RCP scenarios; and (5) quantitatively examine the complex influence of land use and climate change on water retention services in the Loess Plateau. This study furthers our understanding of the relationship between local water and land resources and the results can provide scientific support for regional ecosystem management in the Loess Plateau.

2 Materials and methods

2.1 Study area

The Loess Plateau (33°41′–41°16′N and 100°52′–114°33′E) is the largest (approximately 0.64×10^6 km^2) and most concentrated typical loess landform in the world (Fig. 1). It is characterized by a temperate continental monsoon climate, with annual average temperature and annual reference evapotranspiration (ET$_0$) of 3.6℃–14.3℃ and 1060.00 mm, respectively (Li et al., 2012). The region experiences little and highly spatially heterogeneous precipitation that mainly occurs from June to September during rainstorms (Zhang et al., 2014), accounting for 60%–70% of the total annual precipitation in the Loess Plateau and contributing 90% of the annual total sediment load of the Yellow River (Fu et al., 2017).
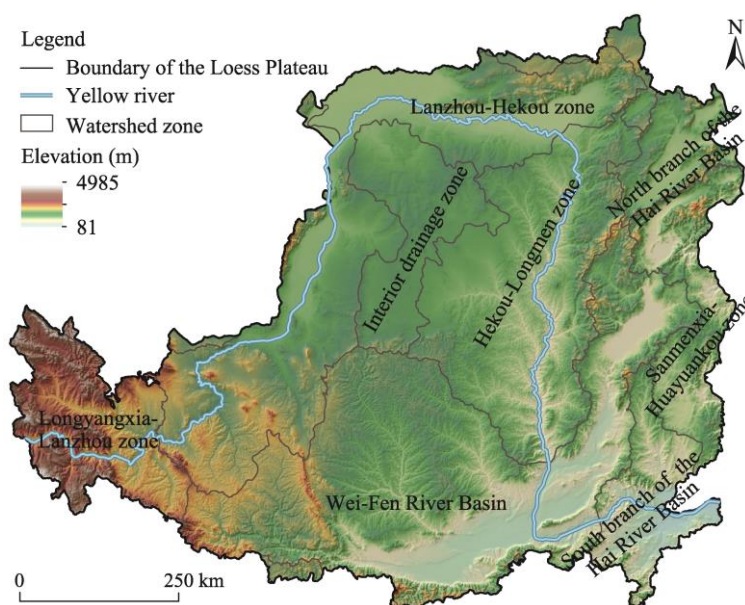

Fig. 1 Overview of the Loess Plateau

In the Loess Plateau, increasing levels of human disturbance (population increasing from less than 40×10^6 in 1949 to over 100×10^6 in 2000; Fu et al., 2017) and continuous climate change have led to serious ecological problems. For example, per capita water availability of the Loess Plateau is only one-fifth of the national average in China. Over-urbanization, over-cultivation, agricultural land abandonment, and vegetation destruction have also accelerated ecological degradation of the Loess Plateau, making it an ecologically fragile area with the most severe water and soil loss in the world (Wang et al., 2018). Since the 1980s, a series of ecological restoration projects (e.g., the TNSFP, NFPP, and GGP) have been initiated in the Loess Plateau, with the aim of alleviating water and soil loss. In 1999–2017, vegetation cover increased by nearly 33% (Lü et al., 2012), however, the negative effects of increased vegetation cover are creating new challenges for regional water resources management in the Loess Plateau. Several studies have pointed out that water demand for increased vegetation cover and canopy ET$_0$ caused by vegetation restoration measures are putting pressure on limited water resources in the Loess Plateau (Sun et al., 2006; Feng et al., 2016a; Shao et al., 2019; Wang et al., 2021). In addition, the large-scale water consumption associated with large-scale urban expansion cannot be ignored, and water resources management activities have become more complex in the context of general temperature rise and precipitation decline in the Loess Plateau (Su and Fu, 2013). Consequently, long-term explicit integrated assessments of water resources in the Loess Plateau are required.

2.2   Methods

Modelling was carried out using the following four steps in this study (Fig. 2). First, summarizing scenarios (HS, EPS, and UES) and potential driving factors (natural environment, socio-economic status, and relevant planning policies in the Loess Plateau) of LUCC as background knowledge. Second, adopting an improved Markov model to predict future land use demands under multiple scenarios (HS, EPS, and UES) based on land use status in the historical period (2000–2015) of the Loess Plateau; utilizing a logistic regression model to evaluate and select factors that potentially drive LUCC; and inputting the driving factors and land use demands into FLUS model to simulate the potential spatial patterns of land use in the future from 2020 to 2050. Third, calculating actual evapotranspiration by integrating soil physical-chemical properties, meteorological data, topographic indices, leaf area index (LAI), and Zhang coefficient (Donohue et al., 2012); and deriving precipitation datasets according to RCP scenarios. Fourth, utilizing Budyko hypothesis to integrate the abovementioned data in the second and third steps to obtain the long-term evaluation results of water retention services in the historical period (2000–2015) and the multi-scenario simulation results of water retention services in the future (2020–2050) in the Loess Plateau.
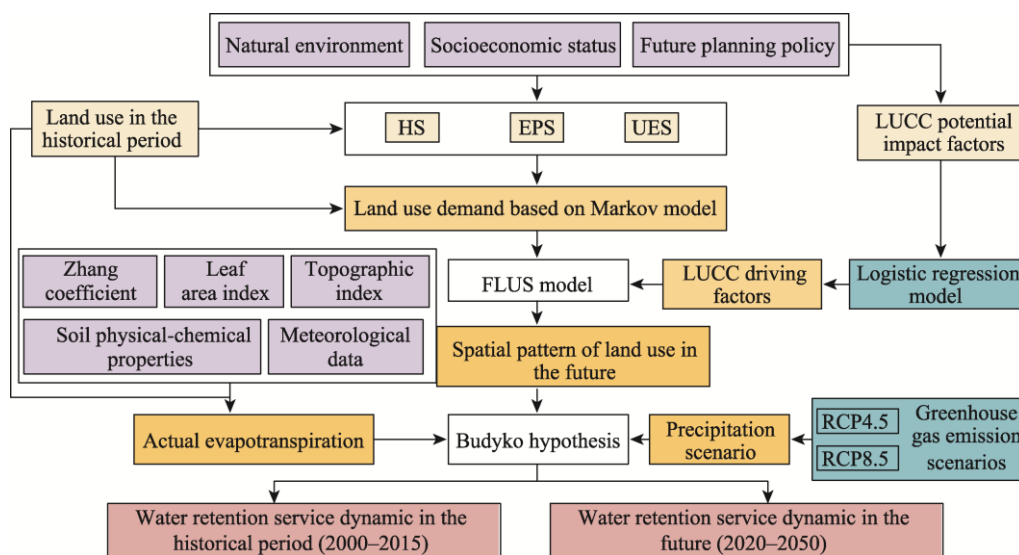
Fig. 2   Integrated modelling framework in this study. HS, historical scenario; EPS, ecological protection scenario; UES, urban expansion scenario; LUCC, land use/cover change; FLUS, future land use simulation; RCP, representative concentration pathway.

2.2.1   Data sources

Multi-source data used to assess water retention services in the Loess Plateau are shown in Table S1. Among them, land use/cover dataset was processed using the European Space Agency (ESA) (https://www.esa-landcover-cci.org) product classification scheme. The ESA climate change initiative dataset, which uses machine learning and unsupervised algorithms, was able to fuse 3.0×10^9 consecutive land cover maps, and the accuracy of the dataset has been verified on a global scale (Li et al., 2018). We reclassified the land use/cover dataset into 10 categories (agricultural land, evergreen broad-leaved forest, deciduous broad-leaved forest, evergreen coniferous forest, closed forest, grassland, shrubland, urban land, water bodies, and others) according to the principles of land iteration efficiency and the data used to support local land management planning; in particular, the area of deciduous coniferous forest was small, therefore, it was classified as closed forest. Digital elevation model (DEM) and the spatial distributions of population and GDP (gross domestic product) were derived from the Resource and Environment Data Cloud Platform, the Chinese Academy of Sciences (http://www.resdc.cn/Default.aspx). Soil attribute data were from the

Environmental and Ecological Science Data Center for West China (http://westdc.westgis.ac.cn/). Precipitation data (2000–2015) and other meteorological data (including temperature, relative humidity, barometric pressure, wind direction speed, and sunshine hours) during 1950–2015, which were mainly used to calculate ET_0, were obtained from the China Meteorological Data Service Center (http://data.cma.cn/), and their spatial distributions were derived using ordinary kriging interpolation method. LAI dataset was extracted from Land-Atmosphere Interaction Research Group at Sun Yat-sen University, China (http://globalchange.bnu.edu.cn/). Future climate data were generated on the basis of the National Aeronautics and Space Administration (NASA) Earth Exchange Global Daily Downscaled Projections (NEX-GDDP) dataset. NEX-GDDP couples the measured values of global sites and data of 21 types of general circulation models (GCMs) in Coupled Model Inter Comparison Project Phase 5 (CMIP5); the dataset includes three climatic variables: daily precipitation, daily maximum temperature, and daily minimum temperature, for the periods of 1950–2005 (historical run) and 2006–2100 (RCP4.5 and RCP8.5 runs) (van Vuuren et al., 2011). Studies have demonstrated that NEX-GDDP can successfully reproduce the spatial patterns of extreme precipitation in China (Chen et al., 2017). Specifically, RCP4.5 and RCP8.5 represent an intermediate scenario and an extreme scenario where policy interventions maintain greenhouse gas emissions below 4.5 and 8.5 W/m^2, respectively. Under RCP4.5 and RCP8.5 scenarios, the global average surface temperature is predicted to increase by 0.9°C–2.0°C and by 1.4°C–2.6°C, respectively (Meinshausen et al., 2011). The grid data were downscaled to a global spatial resolution of 0.25°×0.25° (Raghavan et al., 2018; Sahany et al., 2019) and projected under "Krasovsky_1940_Albers" with a resampled resolution of 1 km. All the data mentioned above were mainly processed using ArcGIS 10.2 software.

2.2.2 Scenario designs

Conflicts between agricultural land protection and urbanization are major challenges to land use management in the Loess Plateau. Rapid urbanization promotes intensive socio-economic development; however, large areas of agricultural land and unused land are occupied, leading to potential challenges such as rural hollowing (Fu et al., 2018). Additionally, ecological restoration projects may reduce available water resources (Liang et al., 2015).

To clarify these complex trade-off relationships mentioned above, we designed three typical LUCC scenarios based on the interactions among agricultural land, urban land, closed forest, and grassland under the influence of climate change in the future (2020–2050) in the Loess Plateau. Scenario 1 (HS) is that the variation trends and rates of different land use types are the same as those in the historical period (2000–2015). Scenario 2 (EPS) moderately slows the degradation of agricultural land, expediates the expansion of forest land and grassland under the closure management, and limits the expansion of urban land; specially, the coverage of closed forest and grassland increases 1.2 times faster while agricultural land decreases 0.8 times more slowly than those under HS. Scenario 3 (UES) is that urban land expansion is rapid and becomes uncontrollable, resulting in less effective ecological restoration under this scenario; specially, the rates of urban land expansion and vegetation coverage increase are 1.2 and 0.9 times of those under HS, respectively.

Because of the difficulty in reducing greenhouse gas emissions with the current socio-economic development condition (Okkan and Kirdemir, 2016), RCP4.5 and RCP8.5 were used to simulate the potential effects of LUCC on water retention services under current and extreme greenhouse gas emission scenarios in the Loess Plateau.

Overall, we created six scenarios by combining land use scenarios (HS, EPS, and UES) and climate change scenarios (RCP4.5 and RCP8.5): RCP4.5-HS, RCP4.5-EPS, RCP4.5-UES, RCP8.5-HS, RCP8.5-EPS, and RCP8.5-UES.

2.2.3 LUCC simulation

(1) Improved Markov-CA model. The prediction results of Markov-CA model are only related to the conversion probability matrix of two periods of land use maps, which have no aftereffect (Guan et al., 2011). Scenario weight matrix based on the initial state transition probability which reflects the

conversion intensities of different land use types relative to their initial states in specific policy scenarios, was introduced to control the multi-scenario expansion simulation capabilities of different land use types.

The improved Markov-CA equations are as follows:

$$P_{(n)} = P_{(n-1)} \times P''_{ij},$$ (1)

$$P'_{ij} = \begin{bmatrix} P_{11} & P_{12} & \cdots & P_{1j} \\ P_{21} & P_{22} & \cdots & P_{2j} \\ \vdots & \vdots & \ddots & \vdots \\ P_{i1} & P_{i2} & \cdots & P_{ij} \end{bmatrix},$$ (2)

$$P''_{ij} = \begin{bmatrix} \dfrac{1}{P'_{11} + P'_{12} + \cdots + P'_{1j}} & & & \\ & \dfrac{1}{P'_{21} + P'_{22} + \cdots + P'_{2j}} & & \\ & & \ddots & \\ & & & \dfrac{1}{P'_{i1} + P'_{i2} + \cdots + P'_{ij}} \end{bmatrix} P'_{ij},$$ (3)

where $P_{(n)}$ is the transition probability matrix of land use types; n is the number of land use types; P'_{ij} is the modified matrix of the initial state probability matrix P_{ij} after the introduction of scenario weight matrix to change the weights of different land use types; and P''_{ij} is the standardized P'_{ij}, which ensures the sum of the conversion probabilities of Equation 3.

(2) FLUS model. We entered the selected land use driving factors using logistic regression and ROC (receiver operating characteristic; its value indicates a better effect when it is greater than 0.7) analysis (Eq. 4; Pontius and Schneider, 2001) into ANN-SPE model to calculate the probabilities of occurrence for different land use types. Afterward, we adopted SAICM model to improve the randomness of LUCC and increase the accuracy of land use pattern simulations (Liu et al., 2017; Liang et al., 2018). The parameterization of FLUS in the Loess Plateau has been completed in the existing study (Sun and Liang, 2021). Then, we used overall accuracy (OA) and Kappa coefficient to assess the accuracy of land use pattern simulations (Pontius and Schneider, 2001; Rwanga and Ndambuki, 2017), where the situation of Kappa coefficient value higher than 0.8 and OA value higher than 0.8 indicates a reasonably high accuracy (Pontius, 2000; Sun and Liang, 2021). LUCC simulations were completed when land use demands are met.

$$\ln\left(\frac{P_i}{1 - P_i}\right) = \alpha + \sum_{i=1}^{n} \beta_i x_i,$$ (4)

where P_i denotes the probability that land use type i is present in the grid of interest; α is the intercept; β_i is the regression coefficient of the ith driving factor; and x_i is the ith driving factor.

(3) Trade-off. We utilized partial correlation analysis to quantitatively explain the trade-off or synergic relationships of specific LUCCs by SPSS software (International Business Machines Corporation, Armonk, New York, United States) (Eqs. 5 and 6). The correlation coefficient values of higher than, lower than, and equalling to zero indicate that variables exhibit trade-off relationship, synergic relationship, and no relationship, respectively (Howe et al., 2014). All the results were subjected to the t-tests.

$$r_{ij} = \frac{\sum_{y=1}^{y} \left(L_{y(i)} - \overline{L_i}\right)\left(L_{y(j)} - \overline{L_j}\right)}{\sqrt{\sum_{y=1}^{y} \left(L_{y(i)} - \overline{L_i}\right)^2 \left(L_{y(j)} - \overline{L_j}\right)^2}},$$ (5)

$$r_{ijk} = \frac{r_{ij} - r_{ik}r_{jk}}{\sqrt{\left(1 - r_{ik}^2\right)\left(1 - r_{jk}^2\right)}}, \tag{6}$$

where r_{ij} is the correlation coefficient between land use type i and land use type j; y is the year; $L_{y(i)}$ and $L_{y(j)}$ represent the area of land use type i and land use type j in a particular year y (km^2), respectively; $\overline{L_i}$ and $\overline{L_j}$ represent the average area of land use type i and land use type j in the study period (km^2), respectively; r_{ijk} is the partial correlation coefficient between land use type i and land use type j when the influence of land use type k is controlled; r_{ik} is the correlation coefficient between land use type i and land use type k; and r_{jk} is the correlation coefficient between land use type j and land use type k . The eighth-order partial correlation coefficient between land use type i and land use type j was progressively obtained when the other eight land use types were simultaneously controlled.

2.2.4 Water retention services assessment

Based on Budyko hypothesis (Donohue et al., 2012) and annual precipitation data, we calculated regional water yield (mm), i.e., the difference between precipitation and AET (transpiration by vegetation and evaporation from the ground surface) (Sun et al., 2006), as follows:

$$\text{Yield} = P - AET, \tag{7}$$

where P is the annual precipitation (mm); and AET is the actual evapotranspiration (mm), which was calculated from the original parameters such as ET$_0$, LAI, and Zhang coefficient. Especially, the annual precipitation amount and frequency (N) data from 133 weather stations in the study area were collected, the annual average Z-value for each station was calculated (Z=0.2N; Donohue et al., 2012), and the ordinary kriging interpolation was performed.

Water retention (mm) was calculated using water yield, topography, soil retention properties, and soil texture, as follows (Wang et al., 2019):

$$\text{Water retention} = \min\left(1, \frac{249}{V}\right) \times \min\left(1, \frac{0.9 \times TI}{3}\right) \times \min\left(1, \frac{K_{sat}}{300}\right) \times \text{Yield}, \tag{8}$$

where V is the dimensionless flow velocity coefficient that reflects the water flow resistance; TI is the topographic index; and K_{sat} is the soil saturated hydraulic conductivity (cm/d) calculated with the help of Neuro Theta (Minasny and McBratney, 2002) using sand, silt, and clay contents of soil.

3 Results

### 3.1 Land use simulations and trade-off analysis

3.1.1 Spatial-temporal changes of land use types

ROC analysis revealed that the driving factors (slope, aspect, precipitation, temperature, population, GDP, distance to cities, roads, railways, and rivers) (Sun and Liang, 2021) in all logistic equations greatly explained the variations in LUCCs, and that evergreen broad-leaved forest and agricultural land had the highest (0.962) and lowest (0.738) ROC values, respectively. The land use maps of 2011–2015 were used to analyze the simulation accuracy of FLUS model, and Kappa coefficient and OA values were in the ranges of 0.801–0.821 and 0.813–0.886, respectively. These results suggested that LUCC simulation with the calibrated LUCC model was spatially consistent and accurate.

The overall patterns in the major LUCCs are relatively consistent under different scenarios in the future (2020–2050), however, distinct variations are observed in several regions. Under UES, the rapid expansion of urban land (0.63×10^3 km^2/a) mainly occurs in the southern part, and the reduction of agricultural land (0.58×10^3 km^2/a) is also noticed. Under EPS, grassland increases significantly (0.20×10^3 km^2/a), while deciduous c, evergreen coniferous forest, and closed forest all expand to varying degrees. The LUCC under HS shows a medium situation between the two scenarios mentioned above. Overall, agricultural land is predicted to shrink by 5.55%–7.39%, and is mainly observed in the central hilly-gully regions (Fig. 3), while urban land is predicted to

increase by 1.34–2.20 times. However, the complex feedback relationship between urbanization and socio-ecological system still requires further investigation in the Loess Plateau.
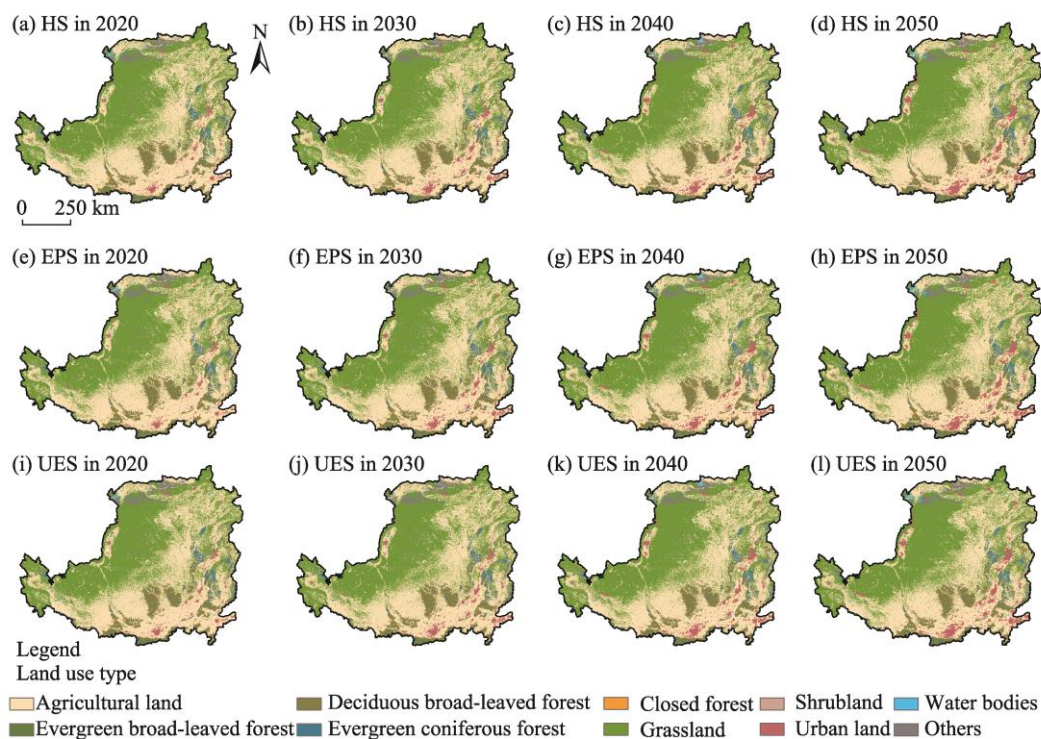

Fig. 3　Simulations of land use type patterns under historical scenario (HS), ecological protection scenario (EPS), and urban expansion scenario (UES) in the Loess Plateau in 2020 (a, e, i), 2030 (b, f, j), 2040 (c, g, k), and 2050 (d, h, l)

3.1.2　Land use conversion and trade-offs

The spatial-temporal variations of land use types shown in Figure 4 demonstrate frequent conversions among agricultural land, urban land, and grassland in the future (2020–2050). Conversions from agricultural land to urban land in the south of the Loess Plateau mainly occur in existing cities and provincial capitals, especially under UES. Areas of agricultural land growth intersect with areas of agricultural land reduction under HS. However, under EPS, local and concentrated growth or shrinkage of agricultural land is noted. Under UES, significant reductions of agricultural land are observed locally, especially the conversion to urban land. Under EPS, the growth intensity of grassland in the north of the Loess Plateau is not substantial, which further supports the expectation regarding to the protection of grassland and closed forest. In contrast, the increase of urban land pixels varies considerably under different scenarios, i.e., UES>HS>EPS, which possibly strengthens the conversion intensity in the surrounding areas and thus reduces crop production for the residents in these cities.

　　The conversions of agricultural land, grassland, and urban land are noticeable (Fig. 4). Under all scenarios, urban land is predicted to expand and occupy agricultural land and other land use types. Grassland is predicted to increase in its area under both EPS and UES, and exhibits a trade-off relationship with deciduous broad-leaved forest but a synergic relationship with closed forest (Fig. S1). Additionally, closed forest shows the most rapid growth under EPS, and conversions between grassland and closed forest occur under all scenarios. Lastly, the others show trade-off relationships with grassland and urban land. The conversion of trade-off relationships among urban land, agricultural land, and ecological land (evergreen broad-leaved forest, deciduous broad-leaved forest, evergreen coniferous forest, closed forest, and grassland) to synergic relationships remains a complex challenge for regional land management.
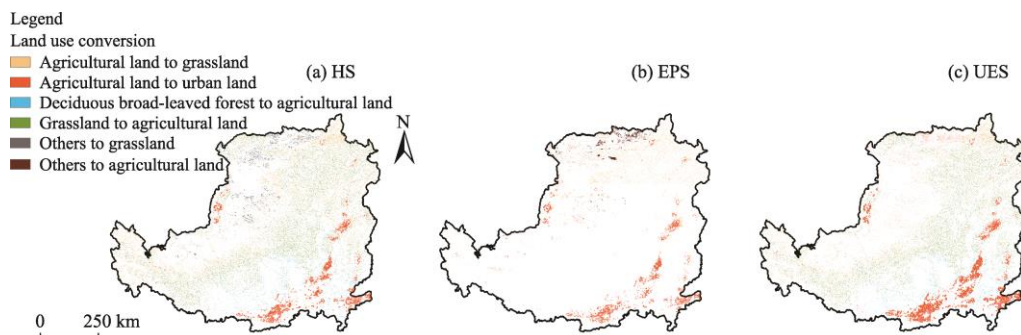
Fig. 4 Conversions of land use types under HS (a), EPS (b), and UES (c) in the Loess Plateau during 2020–2050

3.2 Variations in water retention services

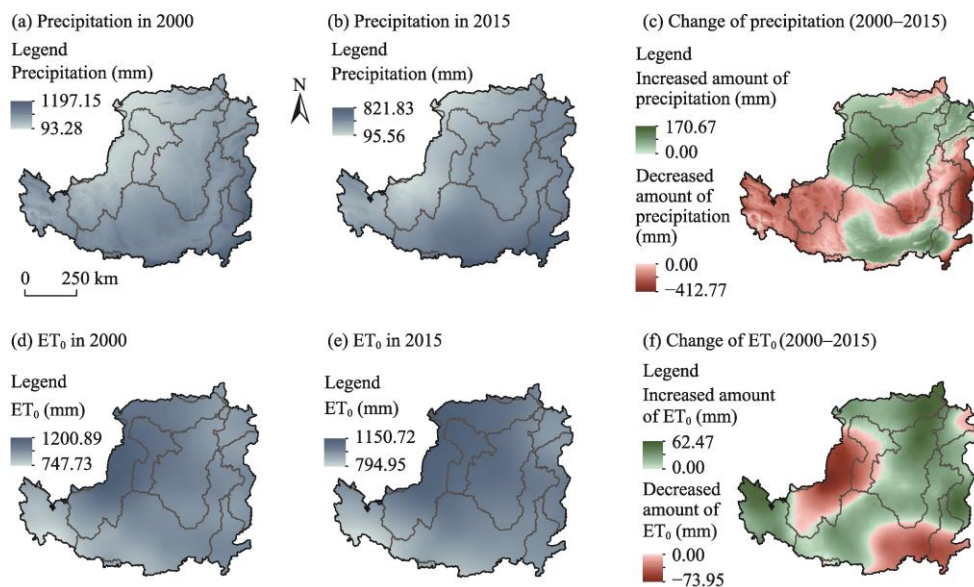### 3.2.1 Spatial-temporal changes of precipitation and ET_0

In 2000–2015, both total precipitation and total ET_0 in the Loess Plateau changed smoothly (Fig. 5). The fluctuation range of precipitation was relatively large, and a negative correlation existed between the trend of precipitation and the trend of ET_0 (correlation coefficient of –0.673; $P<0.05$).
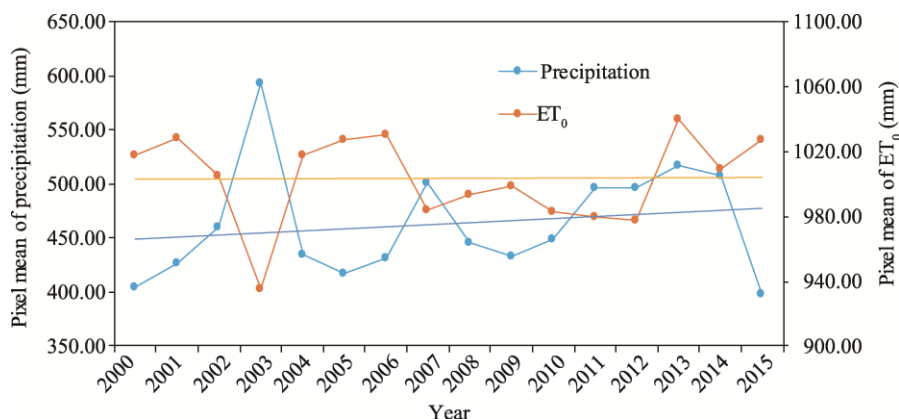
Fig. 5 Time series changes of pixel mean of precipitation and pixel mean of reference evapotranspiration (ET_0) in the Loess Plateau from 2000 to 2015

The average annual precipitation generally decreased from southeast to northwest in the Loess Plateau (Fig. 6a and b). The maximum values of 1197.15 mm in 2000 and 821.83 mm in 2015 were observed in the Wei-Fen River Basin, and the minimum values of 93.28 mm in 2000 and 95.56 mm in 2015 were found in the Lanzhou-Hekou zone. This variation was correlated with altitude. During 2000–2015, the variation of precipitation was significant (Fig. 6c), and the areas with reduced precipitation extended from the middle to the east and west, especially in the Longyangxia-Lanzhou zone and Sanmenxia-Huayuankou zone, with the largest reduction of 412.77 mm. The areas with increased precipitation were mainly located in the north of the Loess Plateau, involving the Lanzhou-Hekou zone, Interior drainage zone, Hekou-Longmen zone, and north branch of the Haihe River Basin, and were also distributed in the south of the Wei-Fen River Basin, with a maximum increase of 170.67 mm.

The average annual ET_0 was generally high in the north and low in the south of the Loess Plateau (Fig. 6d and e). The maximum values were 1200.89 mm in 2000 and 1150.72 mm in 2015, and the high values were concentrated in the Lanzhou-Hekou zone and Interior drainage zone. Obvious boundaries were observed between the areas with increasing and decreasing ET_0 changes (Fig. 6f), and the decrease mainly occurred in the Wei-Fen River Basin and south branch of the Haihe River Basin in the southeast of the Loess Plateau and the Lanzhou-Hekou zone in the northwest of the Loess Plateau, with a maximum decrease of 73.95 mm.

Fig. 6 Spatial distributions and changes of precipitation (a, b, c) and ET_0 (d, e, f) in the Loess Plateau from 2000 to 2015

3.2.2 Spatial-temporal changes of water retention services in 2000–2015

In 2000–2015, the fluctuating changes of water yield and water retention were consistent in the Loess Plateau (Fig. 7), and the peak values occurred in 2003, 2007, and 2012, among which the peak value in 2003 was the highest (158.30×10^6 mm in the Loess Plateau). From 2000 to 2015, water yield decreased by 17.20×10^6 mm, while water retention increased by 0.09×10^6 mm, indicating that vegetation restoration measures such as the GGP exerted positive ecological effects.
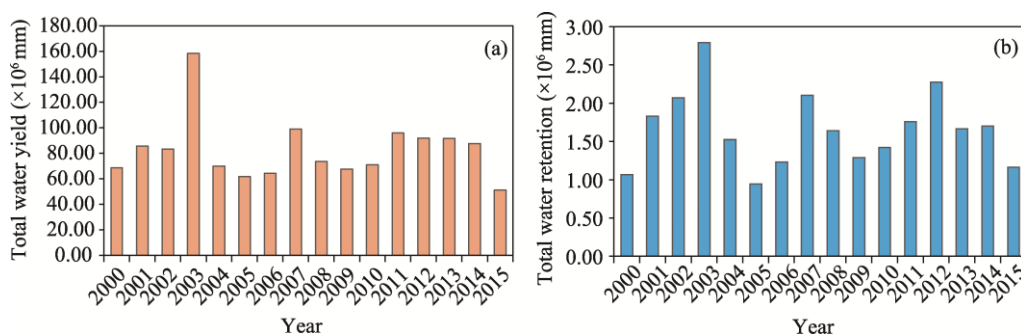

Fig. 7 Time series changes of total water yield (a) and total water retention (b) in the Loess Plateau from 2000 to 2015

In 2000 and 2015, the spatial distribution of water yield was roughly the same, with the high-value areas mainly concentrated in the plains of the Wei-Fen River Basin, north branch of the Haihe River Basin, and south branch of the Haihe River Basin in the Loess Plateau (Fig. 8a and b). During this period (2000–2015), the area where water yield increased was mainly located in the north of the Loess Plateau (Fig. 8c), and the Interior drainage zone and its surrounding areas, which have experienced long-term large-scale vegetation restoration measures (Chen et al., 2015) to convert arid deserts and deserts to oases in the recent years. However, water yield in the southern part mainly decreased.

In addition, the spatial distribution of water retention has undergone major changes during 2000–2015 (Fig. 8d–f), and there were significant changes in the north of the Interior drainage

zone and south of the Wei-Fen River Basin. Especially, high values of water retention were observed in the Interior drainage zone and its surrounding areas. Although the pixel mean of water retention in the Interior drainage zone increased by 1.93 mm, its value in the Loess Plateau decreased by 0.65 mm.
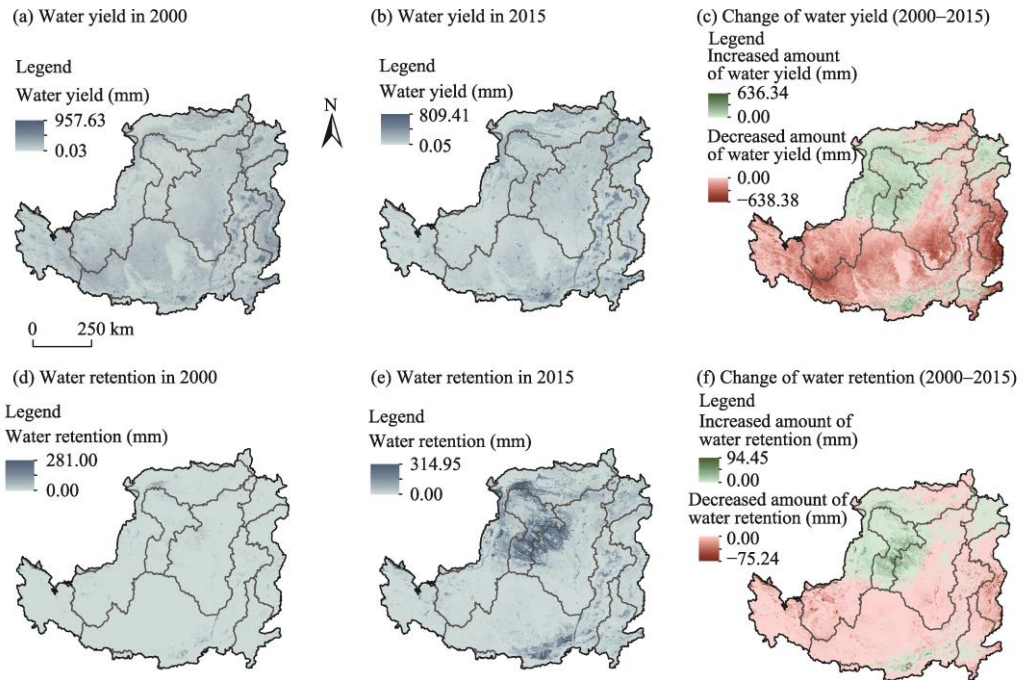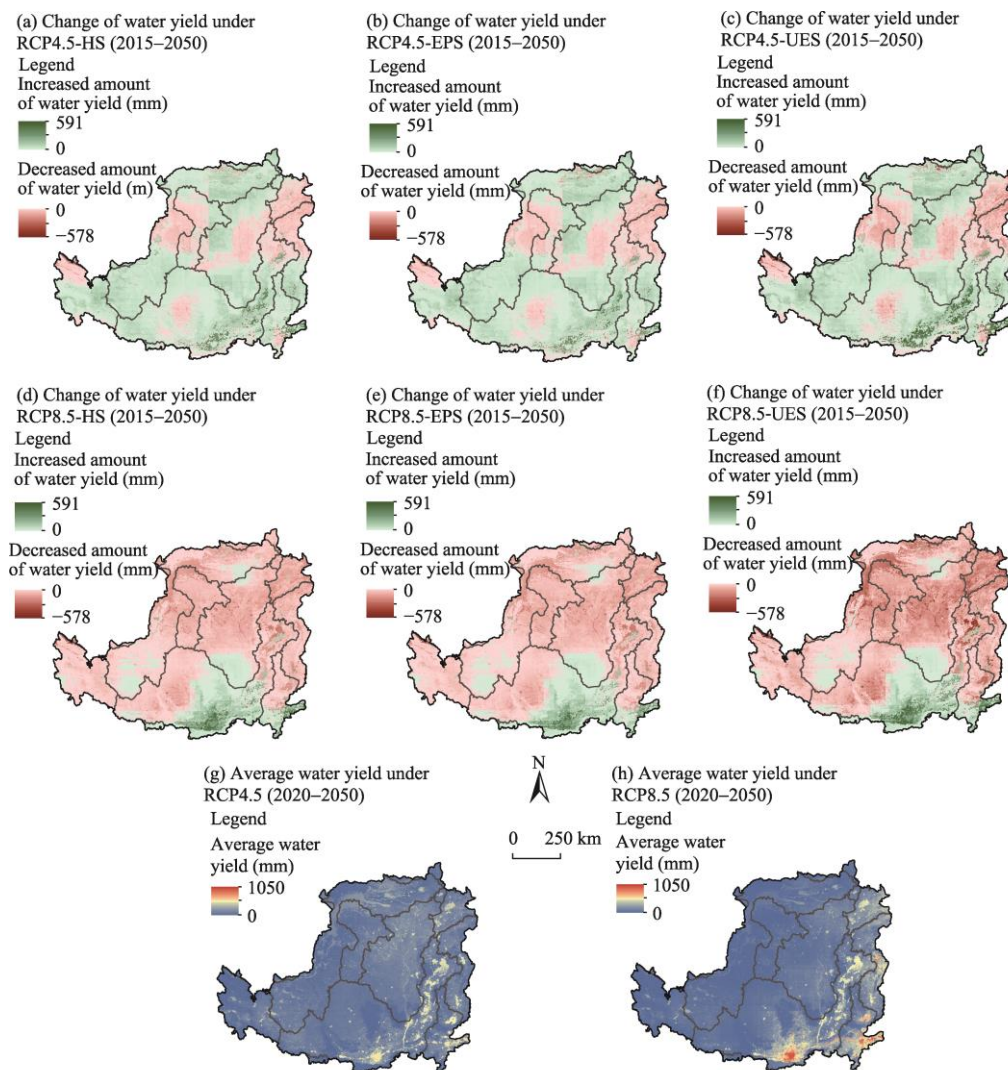
Fig. 8 Spatial distributions and changes of water yield (a, b, c) and water retention (d, e, f) in the Loess Plateau from 2000 to 2015

3.2.3 Spatial-temporal changes of water retention services in 2020–2050

In the simulation period (2020–2050), the multi-year average water yield in the Loess Plateau has the same spatial distribution patterns under two RCP scenarios (Fig. 9), and the high values are distributed in the southern plain of the Wei-Fen River Basin and the south branch of the Haihe River Basin. Water yield values are more prominent under RCP8.5 scenario, with a maximum pixel mean of 1050.00 mm. The spatial distributions of the multi-year average water retention values are different under two RCP scenarios (Fig. 10). Under RCP4.5 scenario, the south of the Wei-Fen River Basin, and the Interior drainage zone and its surroundings are the main areas with high values of water retention, with a maximum pixel mean of 277.46 mm. Under RCP8.5 scenario, the high values are mainly located in the south of the Wei-Fen River Basin, with a maximum pixel mean of 330.20 mm.

The pixel means of water yield under RCP4.5 and RCP8.5 scenarios are 96.63 and 95.46 mm, respectively. In the future (2020–2050), water yield values under RCP4.5 scenario comparatively resemble those in the historical period (2000–2015), and the distributions of areas with high and low water retention values under RCP4.5 scenario are similar to those in the historical period (Fig. 8). Under RCP8.5 scenario, the higher water retention values in the north of the Loess Plateau are considerably reduced and the total water retention decreases by 0.76×10^6 mm compared with that under RCP4.5 scenario. In addition, the percentage of pixel areas where water yield shows an increasing trend decreases with the order of RCP4.5-UES (71.57%)>RCP4.5-HS (71.33%)>RCP4.5-EPS (71.15%)>RCP8.5-UES (22.35%)>RCP8.5-HS (22.29%)>RCP8.5-EPS (22.22%); and the percentage of pixel areas where water retention shows an increasing trend decreases with the order of RCP4.5-HS (70.89%)>RCP4.5-EPS (70.88%)>RCP4.5-UES (70.78%)>RCP8.5-EPS (22.02%)>RCP8.5-HS (21.97%)>RCP8.5-UES (21.87%). For different

land use scenarios, there is a greater and more concentrated increase in water yield in the southeast of the Loess Plateau under UES (the standard deviations of the increased pixels for RCP4.5-UES and RCP8.5-UES are 80.97 and 170.28 mm, respectively), followed by HS (the standard deviations of the increased pixels for RCP4.5-HS and RCP8.5-HS are 61.46 and 143.97 mm, respectively), and the increase in water yield under EPS is more balanced (the standard deviations of the increased pixels for RCP4.5-EPS and RCP8.5-EPS are 61.46 and 86.00 mm, respectively).
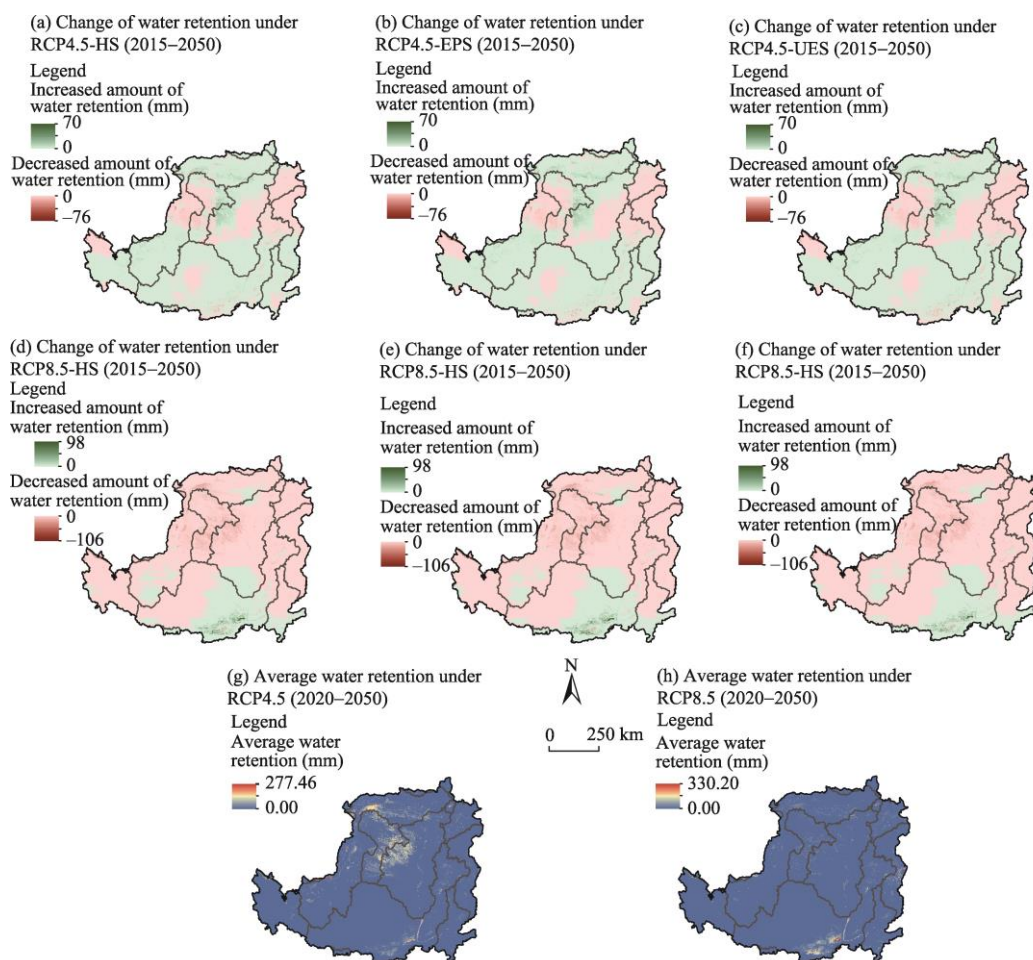

Fig. 9 Spatial distributions and changes of water yield under different scenarios (RCP4.5-HS, RCP4.5-EPS, RCP4.5-UES, RCP8.5-HS, RCP8.5-EPS, and RCP8.5-UES) in the Loess Plateau from 2015 to 2050

At the plateau scale, total water yield values are as follows (in descending order): RCP4.5-UES $(63.80 \times 10^6$ mm)>RCP8.5-UES $(63.10 \times 10^6$ mm)>RCP4.5-HS $(62.50 \times 10^6$ mm)>RCP8.5-HS $(61.70 \times 10^6$ mm)>RCP4.5-EPS $(61.90 \times 10^6$ mm)>RCP8.5-EPS $(61.00 \times 10^6$ mm). Total water yield in the Loess Plateau is 0.76×10^6 mm higher under RCP4.5 scenario than under RCP8.5 scenario. The highest and lowest total water yield values are obtained under UES and EPS, respectively. The findings highlight the importance of increased vegetation cover in the conservation and fixation of water resources. The total water retention values at the plateau scale in descending order are as follows: RCP4.5-EPS $(1.27 \times 10^6$ mm)>RCP4.5-HS $(1.26 \times 10^6$ mm) and RCP4.5-UES $(1.26 \times 10^6$

mm)>RCP8.5-EPS (0.91×10^6 mm)>RCP8.5-HS (0.90×10^6 mm)>RCP8.5-UES (0.89×10^6 mm). Total water retention is 0.37×10^6 mm higher (i.e., more favourable for water retention) under RCP4.5 than under RCP8.5.

Fig. 10 Spatial distributions and changes of water retention under different scenarios (RCP4.5-HS, RCP4.5-EPS, RCP4.5-UES, RCP8.5-HS, RCP8.5-EPS, and RCP8.5-UES) in the Loess Plateau from 2015 to 2050
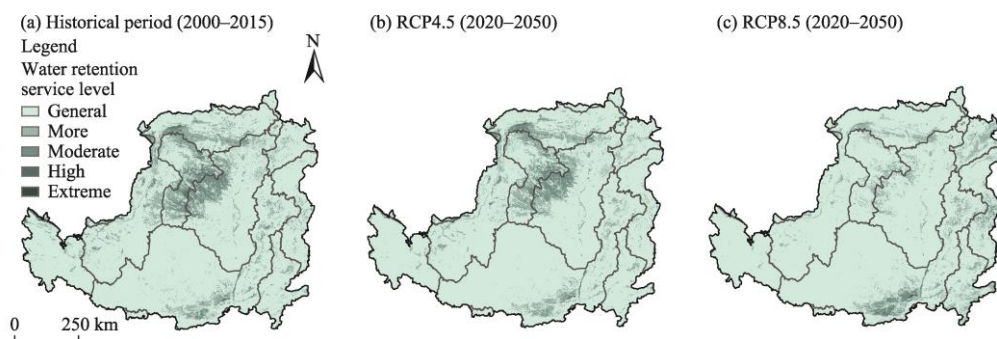
3.2.4 Importance rankings of water retention services

The importance of water retention services in the Loess Plateau in the historical period (2000–2015) and in the future (2020–2050) under RCP4.5 and RCP8.5 scenarios can be divided into five levels (general (0.00–3.00 mm), more (3.00–10.00 mm), moderate (10.00–30.00 mm), high (30.00–80.00 mm), and extreme (80.00–330.20 mm)) using natural breaks method, and the percentages of areas with these different levels were calculated (Table 1). Areas with moderate to high importance levels are mainly located in the northwest of the Lanzhou-Hekou zone, Interior drainage zone, Hekou-Longmen zone, and southern Wei-Fen River Basin (Fig. 11). Under RCP4.5 scenario, 4.33% functional areas have moderate to high importance levels of water retention services, which is 2.23% greater than that under RCP8.5 scenario. Further, under RCP8.5 scenario, the importance levels of water retention services show decreasing trend in the northwest of the Loess Plateau and increasing trend in the south of the Loess Plateau. Functional areas with moderate, high, and extreme importance levels only account for 2.10% of the total area under RCP8.5 scenario. These ranking results may provide reference data for the exploitation of water resources and the determination of priority points and key areas for the enhancement of water retention in the Loess Plateau.

Table 1 Percentage of area with different importance levels of water retention services in the Loess Plateau in the historical period (2000–2015) and in the future (2020−2050) under RCP4.5 and RCP8.5 scenarios

Period	Percentage of area with different importance levels of water retention services (%)				
	General (0–3 mm)	More (3–10 mm)	Moderate (10–30 mm)	High (30–80 mm)	Extreme (80–330.2 mm)
Historical period (2000–2015)	81.29	12.92	5.20	0.59	0.05
Future (2020–2050) under RCP4.5	84.65	11.02	4.03	0.29	0.01
Future (2020–2050) under RCP8.5	88.54	9.36	1.91	0.18	0.01

Note: RCP, representative concentration pathway. The importance of water retention services in the Loess Plateau in the historical period (2000–2015) and in the future (2020–2050) under RCP4.5 and RCP8.5 scenarios can be divided into five levels using natural breaks method: general, 0.00–3.00 mm; more, 3.00–10.00 mm; moderate, 10.00–30.00 mm; high, 30.00–80.00 mm; and extreme, 80.00–330.20 mm.

Fig. 11 Spatial distributions of different importance levels of water retention services in the Loess Plateau in the historical period (2000–2015; a) and in the future (2020–2050; b and c) under RCP4.5 and RCP8.5 scenarios. The importance of water retention services in the Loess Plateau in the historical period (2000–2015) and in the future (2020–2050) under RCP4.5 and RCP8.5 scenarios can be divided into five levels using natural breaks method: general, 0.00–3.00 mm; more, 3.00–10.00 mm; moderate, 10.00–30.00 mm; high, 30.00–80.00 mm; and extreme, 80.00–330.20 mm.

4　Discussion

### 4.1　Correlation between water retention and water yield

Although large-scale vegetation restoration has been carried out in the Loess Plateau, the total amount of water retention is still low in the whole region, and rain retention capacity is very finite. Water retention in the Loess Plateau only accounts for 2.11% of water yield, while water yield accounts for about 24.25% of precipitation. After vegetation restoration, increased water consumption and canopy water consumption consume high amounts of water resources in the Loess Plateau. Trying to obtain high water yield and low water consumption through vegetation restoration and other measures is a challenge. Sun et al. (2006) showed that afforestation measures under the average historical climate conditions in China would decrease runoff at rates of 50.00–150.00 mm/a or with percentages of 20.00%–40.00% in most areas of the country, especially in the Loess Plateau (decreasing rate of 50.00 mm/a or decreasing percentage of 50.00%). According to Lü et al. (2012), after the implementation of the GGP (2000–2008) in the Loess Plateau, runoff in the region decreased at a rate of 10.30 mm/a, and only less than 10.00% of the whole region had increased water yield. In addition, according to Feng et al. (2016a), the massive increase in vegetation after the implementation of the GGP increased net primary productivity (NPP) and ET_0 in the Loess Plateau, and further vegetation expansion could cause regional water shortage. Furthermore, Shao et al. (2019) reported that large-scale vegetation restoration under the implementation of the GGP increased ET_0 significantly (4.39 mm/a) in the Loess Plateau. In 2001–2015, the increase of vegetation under the implementation of the GGP resulted in the consumption of approximately 31.00×10^8 m³/a ET_0. Wang et al. (2021) pointed out

that water retention in the Zhanghe River Basin in the eastern part of the Loess Plateau decreased by 1.10×10^8 m^3/decade from 1960 to 2016, mainly due to increased ecological engineering measures and reduced water consumption by human activities.

Consistent with the results of Feng et al. (2016a), in this study, ET$_0$ was significantly negatively correlated with precipitation, water yield, and water retention, with correlation coefficients of –0.673, –0.720, and –0.737, respectively ($P<0.01$). In the Loess Plateau, the areas with high rates of water retention to water yield were mainly located in the Lanzhou-Hekou zone, Interior drainage zone, and Hekou-Longmen zone in the northwest, with values of 2.58%, 6.25%, and 1.96%, respectively. The complex influences of ecological projects (e.g., the GGP) and the spatial heterogeneity of regions should be comprehensively considered to enable the formulation of suitable ecological measures in the Loess Plateau.

4.2　Variations in water retention services in a typical sandy land area in the Loess Plateau

Increased vegetation coverage in the Loess Plateau has effectively controlled the sediment transport into the Yellow River (Fu et al., 2017). The Mu Us Sandy Land is a typical example; it is one of the major sandy lands in China and is located in the north of central Loess Plateau (Fig. 12). Its harsh ecological environment limits socio-economic development; however, after the implementation of various ecological and environmental governance measures for over 70 a, more than 90.00% of the desertified land is under management (Li et al., 2017; Liu et al., 2020). From 2000 to 2015, 91.75% of area in the Mu Us Sandy Land has increased in water retention, and the total amount of water retention has significantly increased from 0.16×10^6 to 0.37×10^6 mm.
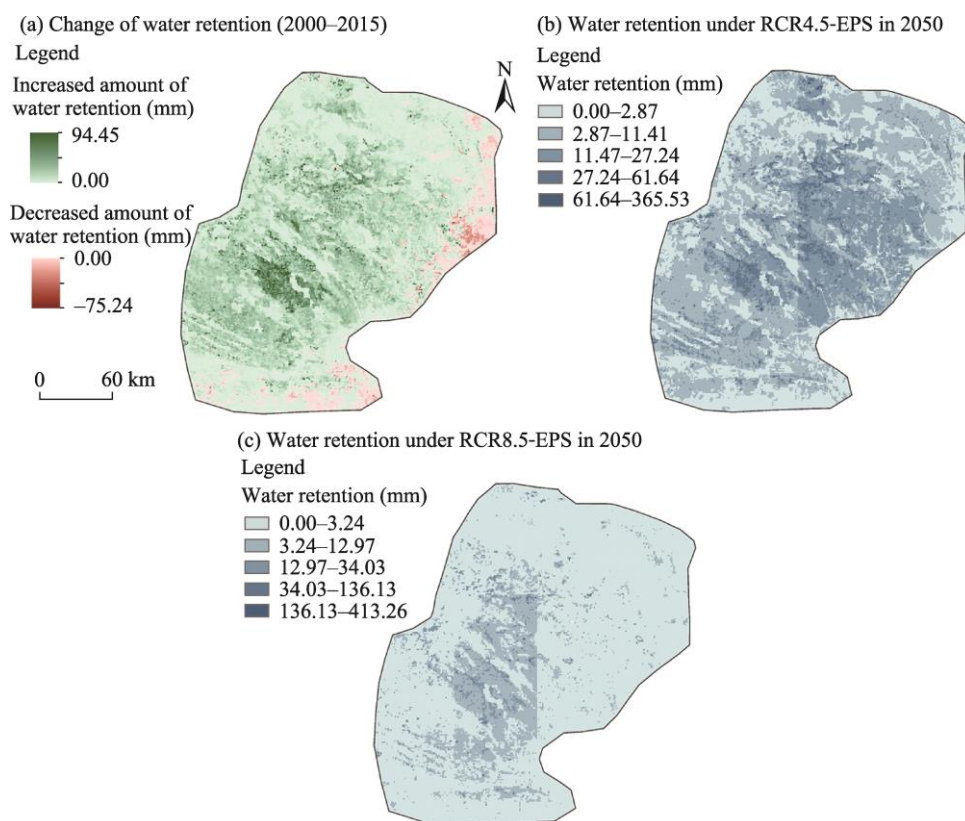
Fig. 12　Spatial distributions of water retention change in the Mu Us Sandy Land in 2000–2015 (a), and spatial distributions of predicted water retention in the Mu Us Sandy Land in 2050 under RCP4.5-EPS (b) and RCP8.5-EPS (c)

Vegetation restoration projects are the key factors that enhance regional water retention services (Liu et al., 2020) and can significantly increase the ecological, social, and economic benefits to the Loess Plateau. Under RCP4.5-EPS, vegetation in the Mu Us Sandy Land is expected to increase continuously, thus considerably promoting water retention. In addition, the total water retention in the Mu Us Sandy Land in 2050 is expected to reach 0.46×10^6 mm, which is much higher than that under RCP8.5-EPS (0.13×10^6 mm). The series of long-term ecological restoration projects have significantly improved the typical ecological environment and enhanced water retention capacity of the Loess Plateau.

4.3 Uncertainty analysis

Integrated modelling methods can facilitate the formulation of land use planning policies that consider both socio-economic development and ecological conservation activities. In this study, we conducted the multi-scenario simulation of water retention services by integrating the LUCC models, water retention assessment, and the spatial mapping methods of intermediate parameters (such as Zhang coefficient), split the process "black box" of mainstream models such as InVEST, and improved the limitation of its constant settings to better depict the actual conditions of the Loess Plateau across multiple climatic zones. Specifically, the improved Markov model was used to predict the land use demand linearly, but in reality, the threshold and inflection point of non-linear change of land use should be taken into consideration, and the simulation based on the FLUS model should further consider the role of policy and so on. Although water retention service assessment was processed to provide an interface for the verification of process parameters, the lack of verification datasets needs to be resolved urgently.

Simulations under six scenarios demonstrated that water yield and water retention in the Loess Plateau are highly consistent with precipitation fluctuations; the average correlation coefficients between water yield and precipitation and between water retention and precipitation are 0.93 and 0.91, respectively, which are consistent with the results of previous studies (Feng et al., 2012; Su and Fu, 2013; Fu et al., 2017). The results of simulation indicate that climate change has a direct and significant impact on water retention services in the Loess Plateau. Moreover, the impact of LUCC and trade-offs cannot be ignored, especially the LUCC caused by two major human activities, i.e., urbanization and vegetation restoration. It is to be noted that, in this study, the forecast of land use demand under different land use scenarios employs a linear calculation process. It can be used as an effort on revealing the greatest impact of different land use/land cover patterns through this more "extreme" forecast, practically along two main development routes of current and future ecological protection and urban land expansion. In addition, quantifying the impacts of LUCC and climate change is an important extension of this study.

5 Conclusions

In the Loess Plateau, the main characteristics of LUCC in the historical period (2000–2015) and in the future (2020–2050) are the mutual conversions among agricultural land, urban land, and grassland. There is a significant trade-off between the expansion of urban land and the decrease of agricultural land. It is thus recommended to strictly control the expansion of cities and towns and to strengthen the conservation and quality improvement of agricultural land and ecological land. In the historical period (2000–2015), the change trends of water yield and water retention are consistent in the Loess Plateau, and the increase of water retention in the Interior drainage zone reflects the effectiveness of vegetation restoration. In the future (2020–2050), the simulated spatial patterns of water yield under two RCP scenarios (RCP4.5 and RCP8.5) are similar in the Loess Plateau, while RCP4.5 model is more conducive to water retention. Compared with HS and UES, water retention under EPS is relatively high. Based on the above findings, we propose that the Loess Plateau should actively explore a new development model that focuses on ecological protection with equal emphasis on quality and benefits on the basis of land intensive development.

Acknowledgements

References

Bai Y, Zhuang C W, Ouyang Z Y, et al. 2011. Spatial characteristics between biodiversity and ecosystem services in a human-dominated watershed. Ecological Complexity, 8(2): 177–183.

Bai Y, Ochuodho T O, Yang J. 2019. Impact of land use and climate change on water-related ecosystem services in Kentucky, USA. Ecological Indicators, 102: 51–64.

Chen H P, Sun J Q, Li H X. 2017. Future changes in precipitation extremes over China using the NEX-GDDP high-resolution daily downscaled data-set. Atmospheric and Oceanic Science Letters, 10(6): 1–8.

Chen J Y, Tao C, Wang H M, et al. 2018. Spatio-temporal evolution of water-related ecosystem services: Taihu Basin, China. PeerJ, 6(3): e5041, doi: 10.7717/peerj.5041.

Chen Y P, Wang K B, Lin Y S, et al. 2015. Balancing green and grain trade. Nature Geoscience, 8: 739–741.

Costanza R, d'Arge R, de Groot R, et al. 1997. The value of the world's ecosystem services and natural capital. Nature, 387: 253–260.

Deng L, Kim D G, Li M Y, et al. 2019. Land-use changes driven by 'Grain for Green' program reduced carbon loss induced by soil erosion on the Loess Plateau of China. Global and Planetary Change, 177: 101–115.

Donohue R J, Roderick M L, McVicar T R. 2012. Roots, storms and soil pores: Incorporating key ecohydrological processes into Budyko's hydrological model. Journal of Hydrology, 436–437: 35–50.

Du X Z, Zhao X, Liang S L, et al. 2020. Quantitatively assessing and attributing land use and land cover changes on China's Loess Plateau. Remote Sensing, 12(3): 353, doi: 10.3390/rs12030353.

Feng X M, Sun G, Fu B J, et al. 2012. Regional effects of vegetation restoration on water yield across the Loess Plateau, China. Hydrology and Earth System Sciences, 16: 2617–2628.

Feng X M, Fu B J, Piao S L, et al. 2016a. Revegetation in China's Loess Plateau is approaching sustainable water resource limits. Nature Climate Chang, 6: 1019–1022.

Feng X M, Cheng W, Fu B, et al. 2016b. The role of climatic and anthropogenic stresses on long-term runoff reduction from the Loess Plateau, China. Science of the Total Environment, 571: 688–698.

Fu B J, Wang S, Liu Y, et al. 2017. Hydrogeomorphic ecosystem responses to natural and anthropogenic changes in the Loess Plateau of China. Annual Review of Earth and Planetary Sciences, 45: 223–243.

Fu W, Lü Y H, Harris P, et al. 2018. Peri-urbanization may vary with vegetation restoration: A large scale regional analysis. Urban Forestry & Urban Greening, 29: 77–87.

Guan D J, Li H F, Inohae T, et al. 2011. Modeling urban land use change by the integration of cellular automaton and Markov model. Ecological Modelling, 222(20–22): 3761–3772.

Hackbart V C S, de Lima G T N P, dos Santos R F. 2017. Theory and practice of water ecosystem services valuation: Where are we going? Ecosystem Services, 23: 218–227.

He G H, Zhao Y, Wang J H, et al. 2019. Attribution analysis based on Budyko hypothesis for land evapotranspiration change in the Loess Plateau, China. Journal of Arid Land, 11(6): 939–953.

Howe C, Suich H, Vira B, et al. 2014. Creating win-wins from trade-offs? Ecosystem services for human well-being: A meta-analysis of ecosystem service trade-offs and synergies in the real world. Global Environmental Change, 28: 263–275.

Hu J Y, Wu Y P, Wang L J, et al. 2021. Impacts of land-use conversions on the water cycle in a typical watershed in the southern Chinese Loess Plateau. Journal of Hydrology, 593: 125741, doi: 10.1016/j.jhydrol.2020.125741.

Hu Y F, Gao M, Batunacun. 2020. Evaluations of water yield and soil erosion in the Shaanxi-Gansu Loess Plateau under different land use and climate change scenarios. Environmental Development, 34: 100488, doi: 10.1016/j.envdev.2019.100488.

Intergovernmental Panel on Climate Change (IPCC). 2017. IPCC Fifth Assessment Report (AR5) Observed Climate Change Impacts Database, Version 2.01. Palisades, NY: NASA Socioeconomic Data and Applications Center (SEDAC). https://doi.org/10.7927/H4FT8J0X.

Jiang C, Zhang H Y, Zhang Z D. 2018. Spatially explicit assessment of ecosystem services in China's Loess Plateau: Patterns, interactions, drivers, and implications. Global and Planetary Change, 161: 41–52.

Kim J S, Choi J S, Choi C L, et al. 2013. Impacts of changes in climate and land use/land cover under IPCC RCP scenarios on

stream flow in the Hoeya River Basin, Korea. Science of the Total Environment, 452–453: 181–195.

Kim S W, Jung Y Y. 2020. Application of the InVEST model to quantify the water yield of North Korean forests. Forests, 11(8): 804, doi: 10.3390/f11080804.

Li B J, Chen D X, Wu S H, et al. 2016. Spatio-temporal assessment of urbanization impacts on ecosystem services: Case study of Nanjing City, China. Ecological Indicators, 71: 416–427.

Li J C, Zhao Y F, Han L Y, et al. 2017. Moisture variation inferred from a nebkha profile correlates with vegetation changes in the southwestern Mu Us Desert of China over one century. Science of the Total Environment, 598: 797–804.

Li W, Macbean N, Ciais P, et al. 2018. Gross and net land cover changes based on plant functional types derived from the annual ESA CCI land cover maps (1992–2015). Earth System Science Data, 10: 219–234.

Li Z, Zheng F L, Liu W Z. 2012. Spatiotemporal characteristics of reference evapotranspiration during 1961–2009 and its projected changes during 2011–2099 on the Loess Plateau of China. Agricultural and Forest Meteorology, 154–155: 147–155.

Liang W, Bai D, Wang F Y, et al. 2015. Quantifying the impacts of climate change and ecological restoration on stream flow changes based on a Budyko hydrological model in China's Loess Plateau. Water Resources Research, 51(8): 6500–6519.

Liang X, Liu X P, Li X, et al. 2018. Delineating multi-scenario urban growth boundaries with a CA-based FLUS model and morphological method. Landscape and Urban Planning, 177: 47–63.

Lin W B, Sun Y M, Nijhuis S, et al. 2020. Scenario-based flood risk assessment for urbanizing deltas using future land-use simulation (FLUS): Guangzhou Metropolitan Area as a case study. Science of the Total Environment, 739: 139899, doi: 10.1016/j.scitotenv.2020.139899.

Liu Q F, Zhang Q, Yan Y Z, et al. 2020. Ecological restoration is the dominant driver of the recent reversal of desertification in the Mu Us Desert (China). Journal of Cleaner Production, 268: 122241, doi: 10.1016/j.jclepro.2020.122241.

Liu X P, Liang X, Li X, et al. 2017. A future land use simulation model (FLUS) for simulating multiple land use scenarios by coupling human and natural effects. Landscape and Urban Planning, 168: 94–116.

Lü Y H, Fu B J, Feng X M, et al. 2012. A policy-driven large scale ecological restoration: Quantifying ecosystem services changes in the Loess Plateau of China. PLoS ONE, 7(2): e31782, doi: 10.1371%2Fjournal.pone.0031782.

Martnez-Harms M J, Balvanera P. 2012. Methods for mapping ecosystem service supply: a review. International Journal of Biodiversity Science, Ecosystem Services & Management, 8(1–2): 17–25.

Meinshausen M, Smith S J, Calvin K, et al. 2011. The RCP greenhouse gas concentrations and their extensions from 1765 to 2300. Climatic Change, 109: 213–241.

Minasny B, McBratney A B. 2002. The Neuro-m method for fitting neural network parametric pedotransfer functions. Soil Science Society of America Journal, 66(2): 352–361.

Muller M R, Middleton J. 1994. A Markov model of land-use change dynamics in the Niagara Region, Ontario, Canada. Landscape Ecology, 9: 151–157.

Ochoa V, Urbina-Cardona N. 2017. Tools for spatially modeling ecosystem services: Publication trends, conceptual reflections and future challenges. Ecosystem Services, 26: 155–169.

Okkan U, Kirdemir U. 2016. Downscaling of monthly precipitation using CMIP5 climate models operated under RCPs. Meteorological Applications, 23(3): 514–528.

Peng J, Shen H, Wu W H, et al. 2016. Net primary productivity (NPP) dynamics and associated urbanization driving forces in metropolitan areas: a case study in Beijing City, China. Landscape Ecology, 31: 1077–1092.

Peng J, Tian L, Liu Y X, et al. 2017. Ecosystem services response to urbanization in metropolitan areas: Thresholds identification. Science of the Total Environment, 607–608: 706–714.

Perrings C, Duraiappah A, Larigauderie A, et al. 2011. The biodiversity and ecosystem services science-policy interface. Science, 331(6021): 1139–1140.

Pontius R G. 2000. Quantification error versus location error in comparison of categorical maps. Photogrammetric Engineering & Remote Sensing, 66(8): 1101–1016.

Pontius R G, Schneider L C. 2001. Land-cover change model validation by an ROC method for the Ipswich watershed, Massachusetts, USA. Agriculture Ecosystems & Environment, 85: 239–248.

Quintas-Soriano C, Castro A J, García-Llorente M, et al. 2014. From supply to social demand: a landscape-scale analysis of the water regulation service. Landscape Ecology, 29: 1069–1082.

Raghavan S V, Hur J, Liong S Y. 2018. Evaluations of NASA NEX-GDDP data over Southeast Asia: present and future climates. Climatic Change, 148: 503–518.

Rwanga S S, Ndambuki J M. 2017. Accuracy assessment of land use/land cover classification using remote sensing and GIS. International Journal of Geosciences, 8: 611–622.

Sahany S, Mishra S K, Salunke P. 2019. Historical simulations and climate change projections over India by NCAR CCSM4: CMIP5 vs. NEX-GDDP. Theoretical and Applied Climatology, 135: 1423–1433.

Shao R, Zhang B Q, Su T X, et al. 2019. Estimating the increase in regional evaporative water consumption as a result of vegetation restoration over the Loess Plateau, China. Journal of Geophysical Research: Atmospheres, 124(22): 11783–11802.

Su C H, Fu B J. 2013. Evolution of ecosystem services in the Chinese Loess Plateau under climatic and land use changes. Global and Planetary Change, 101: 119–128.

Sun D Z, LiangY L. 2021. Multi-scenario simulation of land use dynamic in the Loess Plateau using an improved Markov-CA model. Journal of Geo-information Science, 23(5): 825–835.

Sun G, Zhou G Y, Zhang Z Q, et al. 2006. Potential water yield reduction due to forestation across China. Journal of Hydrology, 328(3–4): 548–558.

van Vliet J. 2019. Direct and indirect loss of natural area from urban expansion. Nature Sustainability, 2: 755–763.

van Vuuren D P, Edmonds J A, Kainuma M, et al. 2011. A special issue on the RCPs. Climatic Change, 109: 1–4.

Wang J F, Wu T L, Li Q, et al. 2021. Quantifying the effect of environmental drivers on water conservation variation in the eastern Loess Plateau, China. Ecological Indicators, 125: 107493, doi: 10.1016/j.ecolind.2021.107493.

Wang S, Fu B J, Chen H B, et al. 2018. Regional development boundary of China's Loess Plateau: Water limit and land shortage. Land Use Policy, 74: 130–136.

Wang Y C, Zhao J, Fu J W, et al. 2019. Effects of the Grain for Green Program on the water ecosystem services in an arid area of China—Using the Shiyang River Basin as an example. Ecological Indicators, 104: 659–668.

Wen X, Théau J. 2020. Spatiotemporal analysis of water-related ecosystem services under ecological restoration scenarios: A case study in northern Shaanxi, China. Science of the Total Environment, 720: 137477, doi: 10.1016/j.scitotenv.2020.137477.

Wu X T, Wang S, Fu B J, et al. 2019. Socio-ecological changes on the Loess Plateau of China after Grain to Green Program. Science of the Total Environment, 678: 565–573.

Zhang B Q, Wu P T, Zhao X N, et al. 2014. Spatiotemporal analysis of climate variability (1971–2010) in spring and summer on the Loess Plateau, China. Hydrological Processes, 28(4): 1689–1702.

Appendix

Table S1 Data sources and data processing used in this study

Name	Source	Format	Period	Processing method
LULC	European Space Agency (https://www.esa-landcover-cci.org)	300 m, grid	2000–2015	Reclassification and resampling
DEM	Resource and Environment Data Cloud Platform, the Chinese Academy of Sciences (http://www.resdc.cn/Default.aspx)	1000 m, grid	2003	Slope, aspect, and catchment calculations by ArcGIS 10.2
Soil properties	Environmental and Ecological Science Data Center for West China (http://westdc.westgis.ac.cn/)	30 s, grid	2013	Projection conversion and resampling
Precipitation	China Meteorological Data Service Center (http://data.cma.cn/)	Text	2000–2015	Data organization and interpolation
	National Aeronautics and Space Administration (NASA) (https://nex.nasa.gov/nex/projects/1356/)	25 km, grid	2020–2050	Format conversion and resampling
Meteorological elements	China Meteorological Data Service Center (http://data.cma.cn/)	Text	2000–2015	Data organization and interpolation
LAI	Land-Atmosphere Interaction Research Group at Sun Yat-sen University, China (http://globalchange.bnu.edu.cn/)	30 s, grid	2000–2015	Projection and resampling
Population, GDP	Resource and Environment Data Cloud Platform, the Chinese Academy of Sciences (http://www.resdc.cn/Default.aspx)	1000 m, grid	2000–2015	Projection
Geographical elements	Resource and Environment Data Cloud Platform, the Chinese Academy of Sciences (http://www.resdc.cn/Default.aspx)	Vector		Projection and data cropping
Catchment boundaries	Resource and Environmental Science Data Center, the Chinese Academy of Sciences (http://www.resdc.cn/data.aspx)	Vector		Projection and data cropping

Note: LULC, land use/land cover; DEM, digital elevation model; LAI, leaf area index; GDP, gross domestic product.

(a) HS

	Agricultural land	Evergreen broad-leaved forest	Deciduous broad-leaved forest	Evergreen coniferous forest	Closed forest	Grassland	Shrubland	Urban land	Water bodies	Others
Agricultural land	1.000	−0.840	−0.981	−0.997	0.000	0.000	−0.898	−1.000	−1.000	0.997
Evergreen broad-leaved forest		1.000	0.021	0.432	0.000	0.000	−0.074	−0.813	0.508	−0.492
Deciduous broad-leaved forest			1.000	0.998	−0.996	0.000	−0.664	0.989	0.505	−0.283
Evergreen coniferous forest				1.000	0.604	0.000	−0.084	−0.823	0.565	−0.782
Closed forest					1.000	0.000	0.903	0.996	0.778	−0.948
Grassland						1.000	0.734	−1.000	−0.827	−1.000
Shrubland							1.000	0.446	0.444	0.962
Urban land								1.000	0.506	−0.921
Water bodies									1.000	−0.578
Others										1.000

(b) EPS

	Agricultural land	Evergreen broad-leaved forest	Deciduous broad-leaved forest	Evergreen coniferous forest	Closed forest	Grassland	Shrubland	Urban land	Water bodies	Others
Agricultural land	1.000	−0.979	−0.924	0.997	−0.999	0.000	0.739	0.000	−0.999	0.979
Evergreen broad-leaved forest		1.000	−0.252	0.161	0.000	−0.231	−0.346	−0.273	0.347	−0.337
Deciduous broad-leaved forest			1.000	0.985	−0.987	0.845	−0.759	0.607	−0.143	0.000
Evergreen coniferous forest				1.000	0.965	−0.964	−0.875	−0.98	0.775	−0.996
Closed forest					1.000	−0.135	0.085	0.984	0.079	−0.375
Grassland						1.000	−0.555	0.794	0.156	−0.896
Shrubland							1.000	0.012	−0.051	0.759
Urban land								1.000	0.411	−0.939
Water bodies									1.000	−0.664
Others										1.000

(c) UES

	Agricultural land	Evergreen broad-leaved forest	Deciduous broad-leaved forest	Evergreen coniferous forest	Closed forest	Grassland	Shrubland	Urban land	Water bodies	Others
Agricultural land	1.000	−0.971	0.858	0.000	−0.35	0.000	−0.602	−1.000	−0.999	0.997
Evergreen broad-leaved forest		1.000	0.960	0.965	−0.908	0.000	0.386	−0.97	−0.481	0.914
Deciduous broad-leaved forest			1.000	0.910	−0.826	0.000	−0.881	−0.241	−0.897	0.017
Evergreen coniferous forest				1.000	0.501	0.000	−0.190	−0.869	0.604	−0.931
Closed forest					1.000	0.000	0.543	0.963	−0.323	−0.805
Grassland						1.000	0.596	−0.999	0.234	−1.000
Shrubland							1.000	−0.309	−0.735	0.927
Urban land								1.000	0.686	−0.875
Water bodies									1.000	−0.624
Others										1.000

Fig. S1 Correlation of different land use types under HS (a), EPS (b), and UES (c) in the Loess Plateau. HS, historical scenario; EPS, ecological protection scenario; UES, urban expansion scenario.